Clinical Neurophysiology 144 (2022) 83–90

Contents lists available at ScienceDirect

Clinical Neurophysiology

journal homepage: www.elsevier.com/locate/clinph

Quantitative pretreatment EEG predicts efficacy of ACTH therapy in infantile epileptic spasms syndrome

Sotaro Kanai [a,*], Masayoshi Oguri [b], Tohru Okanishi [a], Yosuke Miyamoto [c], Masanori Maeda [d], Kotaro Yazaki [e], Ryuki Matsuura [f], Takenori Tozawa [c], Satoru Sakuma [e], Tomohiro Chiyonobu [c], Shin-ichiro Hamano [f], Yoshihiro Maegaki [a]

[a] Division of Child Neurology, Institute of Neurological Sciences, Faculty of Medicine, Tottori University, 86 Nishi-cho, Yonago 683-8503, Japan
[b] Department of Medical Technology, Kagawa Prefectural University of Health Sciences, 281-1 Mure-cho, Takamatsu 761-0123, Japan
[c] Department of Pediatrics, Kyoto Prefectural University of Medicine, 465 Kajii-cho, Kamigyo-ku, Kyoto 602-8566, Japan
[d] Department of Pediatrics, Wakayama Medical University, 811-1 Kimiidera, Wakayama 641-8509, Japan
[e] Department of Pediatrics, Osaka Metropolitan University Graduate School of Medicine, 1-4-3 Asahi-machi, Abeno-ku, Osaka 545-8585, Japan
[f] Division of Neurology, Saitama Children's Medical Center, 1-2 Shintoshin, Chuo-ku. Saitama 330-8777, Japan

ARTICLE INFO

Article history:
Accepted 4 October 2022
Available online 19 October 2022

Keywords:
Infantile epileptic spasms syndrome
Epileptic spasms
West syndrome
ACTH therapy
EEG quantitative analysis

HIGHLIGHTS

- We explored the correlation between adrenocorticotrophic hormone (ACTH) outcomes and pretreatment EEG using quantitative analyses in non-lesional infantile epileptic spasms syndrome (IESS).
- The power and functional connectivity in the lower frequency bands positively correlated with unfavorable seizure outcome.
- This study may provide novel electrophysiological factors to predict the efficacy of ACTH therapy in non-lesional IESS.

ABSTRACT

Objective: This study aimed to determine the correlation between outcomes following adrenocorticotrophic hormone (ACTH) therapy and measurements of relative power spectrum (rPS), weighted phase lag index (wPLI), and graph theoretical analysis on pretreatment electroencephalography (EEG) in infants with non-lesional infantile epileptic spasms syndrome (IESS).
Methods: Twenty-eight patients with non-lesional IESS were enrolled. Outcomes were classified based on seizure recurrence following ACTH therapy: seizure-free (F, n = 21) and seizure-recurrence (R, n = 7) groups. The rPS, wPLI, clustering coefficient, and betweenness centrality were calculated on pretreatment EEG and were statistically analyzed to determine the correlation with outcomes following ACTH therapy.
Results: The rPS value was significantly higher in the delta frequency band in group R than in group F ($p < 0.001$). The wPLI values were significantly higher in the delta, theta, and alpha frequency bands in group R than in group F ($p = 0.007$, <0.001, and <0.001, respectively). The clustering coefficient in the delta frequency band was significantly lower in group R than in group F ($p < 0.001$).
Conclusions: Our findings demonstrate the significant differences in power and functional connectivity between outcome groups.
Significance: This study may contribute to an early prediction of ACTH therapy outcomes and thus help in the development of appropriate treatment strategies.
© 2022 International Federation of Clinical Neurophysiology. Published by Elsevier B.V. All rights reserved.

Abbreviations: EEG, electroencephalography; ACTH, adrenocorticotrophic hormone; rPS, relative power spectrum; wPLI, weighted phase lag index; IESS, infantile epileptic spasms syndrome; WS, West syndrome; DEE, developmental and epileptic encephalopathy; ES, epileptic spasms; HPA, hypothalamus–pituitary–adrenal; AED, antiepileptic drug; F, seizure-free group; R, seizure-recurrence group; C, clustering coefficient; BC, betweenness centrality; ANOVA, analysis of variance; FDR, false discovery rate; ROC, receiver operating characteristic.

* Corresponding author.
E-mail address: s.kanai82@gmail.com (S. Kanai).

https://doi.org/10.1016/j.clinph.2022.10.004
1388-2457/© 2022 International Federation of Clinical Neurophysiology. Published by Elsevier B.V. All rights reserved.

1. Introduction

Infantile epileptic spasms syndrome (IESS), including the classically called West syndrome (WS), is a common developmental and epileptic encephalopathy (DEE) with a number of hypotheses for its etiology (Fusco et al., 2020; Pavone et al., 2020; Zuberi et al., 2022). Patients with IESS typically show three features: epileptic spasms (ES), developmental arrest or regression, and catastrophic abnormalities on electroencephalography (EEG) called hypsarrhythmia (Fusco et al., 2020; Pavone et al., 2020). Globally accepted standard treatments for patients with IESS are adrenocorticotropic hormone (ACTH), oral corticosteroids, and vigabatrin (Pavone et al., 2020; Knupp et al., 2016). Temporary cessation of ES and hypsarrhythmia is achieved in 45–84% of the patients with ACTH therapy, and approximately half of the responders experience recurrence of seizures (Knupp et al., 2016; Paprocka et al., 2022; Daida et al., 2021; Riikonen et al., 2020; Riikonen, 2020). Favorable seizure outcome with normal to near-normal development is confined to approximately 30–40% of patients (Pavone et al., 2020; Paprocka et al., 2022; Bitton et al., 2021).

Few factors are available to predict unfavorable outcomes at the onset of IESS. Gul Mert et al. reported that unfavorable outcomes were associated with symptomatic etiology, young age at onset, and late and inappropriate treatment (Gul Mert et al., 2017). Magnetic resonance imaging (MRI) is considered the most important tool for categorizing etiologies or brain structural abnormalities (Riikonen, 2020). However, in infantile cases showing no structural or acquired abnormalities on MRI, the prediction of treatment outcomes becomes more challenging.

The pathological mechanisms underlying IESS remain largely unknown. Some researchers have hypothesized, based on high-frequency oscillation slow-wave coupling in interictal EEG, that ES and hypsarrhythmia are derived from cortical–subcortical interactions, whereby the cortex triggers the activation of subcortical structures (Iimura et al., 2018; Bernardo et al., 2020). Although several studies have intended to predict outcomes in patients with IESS by investigating changes between pre- and post-treatment EEG using mechanical quantitative analyses (Wang et al., 2021; Uda et al., 2021), having objective markers analyzed in pretreatment EEG to predict treatment responses will be clinically useful.

Epilepsy is now known as a dysfunction in the dynamics of the brain network, which generates seizures by large-scale hypersynchronous activity (Richardson, 2012). Previous studies analyzing EEG power have shown a correlation between the emergence of gamma activity during interictal EEG in patients with WS and the intractableness of seizures (Kobayashi et al, 2015; Baba et al., 2019). The weighted phase lag index (wPLI), a tool to describe the brain network, is widely used for estimating EEG functional connectivity (Ortiz et al., 2012; Imperatori et al., 2019). The brain neuronal network can be captured by the synchrony of rhythmic activity in EEG. Graph theoretical analysis, which is constructed based on wPLI, characterizes the architecture of the neuronal network and has been broadly applied to epilepsy studies (van Diessen et al., 2013; Pegg et al., 2021).

A previous study showed that ACTH levels in the cerebrospinal fluid of patients with ES were significantly lower than those of controls (Baram et al., 1992). Additionally, modifications in diurnal cortisol rhythms have been observed in patients with ES, suggesting a hypothalamus–pituitary–adrenal (HPA) axis dysfunction (Peng et al., 2020). The authors hypothesized that the outcome following ACTH treatment might depend on the degree of HPA axis dysfunction. Although little is known about the mechanisms of the antiepileptic action of ACTH, it is hypothesized to exert its efficacy through the modulation of projections from the subcortical structures, including the raphe areas in the brainstem (Chugani, 2002; Velísek et al., 2007). In this sense, the dysfunction of subcortical structures may project to diffuse cortical areas, such as those regulating the HPA axis, and affect power and functional connectivity of EEG. Therefore, we hypothesized that the efficacy of ACTH therapy may correlate with the power and functional connectivity in the pretreatment EEG in patients with non-lesional IESS. We performed relative power spectrum (rPS), wPLI, and subsequent graph theoretical analyses of pretreatment EEGs and investigated whether any correlation exists with long-term outcomes following ACTH therapy.

2. Materials and methods

2.1. Patients

Patients with IESS were identified from the medical records at Tottori University Hospital, University Hospital Kyoto Prefectural University of Medicine, Wakayama Medical University Hospital, Osaka Metropolitan University Hospital, and Saitama Children's Medical Center. Clinical data and EEG recordings were retrospectively collected from the medical records of each patient.

The inclusion criteria were as follows: (1) having developed ES prior to the age of 1 year; (2) not having presented with any seizure types other than ES prior to their onset; (3) having received ACTH therapy; (4) having an EEG recorded prior to treatment including ACTH, oral steroids, or vigabatrin; (5) having presented hypsarrhythmia on EEG; (6) having presented no apparent epileptogenic structural abnormalities, such as focal cortical dysplasia, lissencephaly, tuberous sclerosis complex, and periventricular leukomalacia, in pretreatment brain MRI; and (7) a follow-up period longer than 12 months after ACTH treatment. Patient information was anonymized prior to the analyses. This study was conducted in accordance with the institutional guidelines of Tottori University. The protocol was approved by the institutional review board. Informed consent was obtained using the opt-out method owing to the retrospective nature of this study.

2.2. Clinical profiles

For each patient, the following clinical data were reviewed: sex, perinatal history, developmental history, etiology, age at ES onset, age at pretreatment EEG, use of sedative agents on EEG recording, prescribed antiepileptic drugs (AEDs) other than ACTH, duration between ES onset and ACTH, dosage and duration of ACTH treatment, post-treatment outcomes of seizures and EEG, and follow-up period. For premature patients (<37 weeks of gestation), the corrected age was applied. The patients were divided into two outcome groups, the seizure-free group (F) and seizure-recurrence group (R), based on whether or not they had experienced seizure recurrence up to the last follow-up. Seizure recurrence included the development of any type of seizure following ACTH treatment, such as ES, tonic seizures, or focal-onset seizures.

2.3. EEG data acquisition and processing

Fig. 1 shows a scheme of the analytical methodology. Scalp video-EEG data were recorded using a Neurofax system (Nihon-Kohden, Tokyo, Japan). EEG electrodes were placed in accordance with the international 10–20 scalp-electrode position. The sampling frequency was set to 200 Hz (patients 1–6, 22, 23, 26, and 27) or 500 Hz (patients 7–21, 24, 25, and 28). Low- and high-cut filters were set at 0.5 and 60 Hz, respectively.

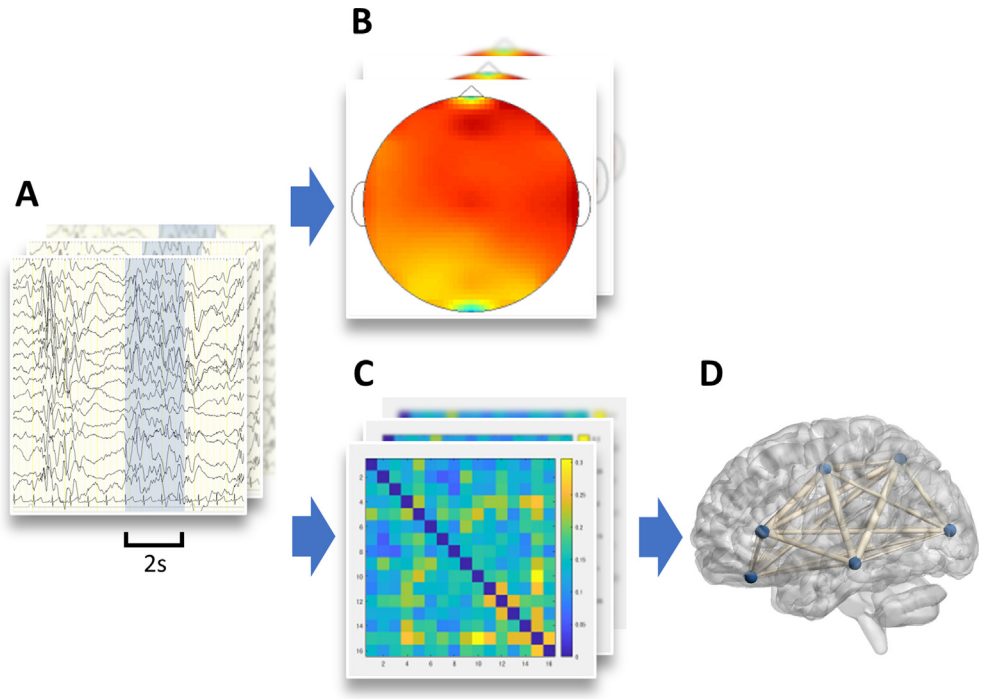

Fig. 1. Overview of the processing steps in rPS, wPLI, and graph theoretical analyses (A) Collecting 34 to 40 epochs of 2-s bursts of hypsarrhythmia from each individual. (B) Calculating power in each epoch, each freXia et al., 2018quency band. A single rPS value was obtained by averaging the values in each individual. (C) Performing wPLI analysis for each epoch, for each frequency band. A single wPLI value was obtained by averaging the values obtained from each individual. (D) Constructing graph measures based on the wPLI matrix data. The image was delineated using BrainNet Viewer (). *Abbreviations:* rPS, relative power spectrum; wPLI, weighted phase lag index.

For the computed analyses, selected EEG data with monopolar montages (Fp1, Fp2, F3, F4, C3, C4, P3, P4, O1, O2, F7, F8, T3, T4, T5, and T6) were used. The average of C3 and C4 was set as the system reference. Considering poor inter-rater agreement in determining hypsarrhythmia, EEG with a Burden of Amplitudes and Epileptiform Discharges score of 4 or greater was determined to be appropriate (Mytinger et al., 2015). A 2-s sleep epoch was randomly selected by two EEG specialists certified by the Japanese Society of Clinical Neurophysiology. Sleep EEG was used to avoid electromyographic artifacts. The starting point of the epoch was set at the root of the initial spike in the periodic burst of hypsarrhythmia, with a duration of more than 2 s. Thirty-four to 40 non-overlapping 2-s epochs were acquired from each patient.

2.4. Relative power spectrums

The powers of each epoch were initially analyzed using individual frequency bands with monopolar montages: delta (0.5–3.9 Hz), theta (4–7.9 Hz), alpha (8–12.9 Hz), beta (13–29.9 Hz), and gamma (30–79.9 Hz). The rPS was calculated with a Hamming window for frequencies between 0.5 and 79.9 Hz, using the MATLAB (MathWorks) plug-in for EEGLAB.

The rPS for each electrode in each frequency band was calculated. Subsequently, the mean value of all epochs was computed to obtain a single rPS value for each frequency band for each patient.

2.5. Weighted phase lag index

A custom Python under Jupiter notebook script was applied to each 2-s epoch. Analyses were performed for each frequency band.

Rhythmic activity has a relevant role in the human nervous systems and has been implicated in numerous functions; oscillatory activity in different brain areas can be synchronized. wPLI is a functional connectivity measure that quantified how consistently 90° (or 270°) phase 'lagging' one EEG signal was compared to another. Before computing the wPLI value, a bandpass filter was used to extract the signal for each band. wPLI measures the extent to which the angle differences between two time series x(t) and y (t) are distributed toward the positive or negative part of an imaginary axis in the complex plane (Vinck et al., 2011):

$$wPLI = \left| \frac{E(|\Delta\phi| \sin(\Delta\phi))}{E|\Delta\phi|} \right|$$

The wPLI is based on the imaginary component of the cross-spectrum and thus implies robustness to noise compared to coherence, as uncorrelated noise sources cause an increasing signal power (Vinck et al., 2011). Different from phase lag index, this procedure reduces the probability of detecting "false-positive" connectivity in the case of volume-conducted noise sources with near zero phase lag and increases the sensitivity in detecting phase synchronization (Peraza et al., 2012). The mean value in each frequency band was computed to obtain a single wPLI coupling value.

2.6. Graph theoretical analysis

Directed and weighted graphs were constructed with electrodes representing nodes, and edges were weighted according to the wPLI matrix data. Subsequently, two commonly used metrics were calculated: the clustering coefficient (C), which is the fraction of triangles around an individual node, and the weighted betweenness centrality (BC), which is the fraction of all shortest paths in the network that pass through it (Rubinov and Sporns, 2010). C is a simple parameter for network segregation describing local interconnectedness, and BC is a measure for network integration detecting anatomical and important functional connections. These metrics were calculated for each participant in each frequency band using Gretna in MATLAB.

2.7. Statistical analyses

Clinical profiles were reported as means and standard deviations. To compare these data, Fisher's exact probability test and Welch's t-test were used, as appropriate.

To correct the skewed distribution of wPLI, the values were log-transformed using the natural logarithm (log wPLI). To clarify the global differences between groups, the values of rPS, log wPLI, C, and BC were compared using a two-way factorial analysis of variance (ANOVA) model across groups F and R: for wPLI, each value and pair of electrodes in each patient were the dependent variables, and for rPS, C, and BC, each value and electrode in each patient were the dependent variables. For pairs of electrodes or electrodes with statistical significance, the Tukey–Kramer method was used as a post-hoc analysis. To evaluate the difference in focality on rPS and wPLI, these values were compared between groups using a two-sided Welch's t-test among all electrodes or pairs of electrodes.

Statistical analyses were performed using the SPSS version 27 (IBM Corp.). Statistical significance was set at $p < 0.05$. For multiple comparisons across multiple rPS, wPLI channels, and both graph measures using two-way factorial ANOVA, the Benjamini–Hochberg false discovery rate (FDR) procedure was applied to correct for the expected proportion of false discoveries (Benjamini and Hochberg, 1995). The q-value for the expected proportion of false discoveries was set at 5% ($q = 0.05$).

3. Results

3.1. Patient demographics

Among 28 (11 male and 17 female) patients who met the inclusion criteria, 21 (75%) were included in group F and seven (25%) in group R. Although one patient presented with mild cerebral atrophy in the bilateral frontal lobes on pretreatment MRI, which was not considered epileptogenic at that time, others did not show brain abnormalities. Regarding the genetic etiology, chromosomal abnormalities were identified in four patients and *STXBP1* pathogenic variant in one, although this was detected 8 months after ACTH therapy. None of the patients presented with seizure types other than ES prior to ACTH therapy. Associations between outcomes and clinical variables are shown in Table 1; no significant associations were found. The detailed patient demographics are presented in Supplementary Table 1.

3.2. Differences on rPS, wPLI, and graph theoretical analysis between groups

Fig. 2 shows the group differences for each analysis. The actual values in the rPS, wPLI, and graph theoretical analyses are shown in Supplementary Dataset 1. The detailed results of the two-way factorial ANOVA are shown in Supplementary Table 2.

The rPS demonstrated significantly higher power in the delta frequency band in group R than in group F ($p < 0.001$), although the power in the theta, alpha, beta, and gamma bands was significantly lower ($p < 0.001$, $p = 0.015$, $p < 0.001$, and $p < 0.001$, respectively). Log wPLI values demonstrated significantly higher connectivity in group R than in group F in the delta, theta, and alpha frequency bands ($p = 0.007$, $p < 0.001$, and $p < 0.001$, respectively). Graph theoretical analyses revealed a significantly lower C in the delta frequency band in group R than in group F ($p < 0.001$), whereas BC showed no significant differences across all frequency bands. Although electrode variables in the theta frequency band on rPS and BC showed significant differences, post-hoc analysis revealed significant differences only between Fp2 and P3 on rPS ($p = 0.025$). No significant differences were found in the interaction effects.

To validate the local distribution of rPS and wPLI, Welch's t-test was implemented between groups across all electrodes on rPS or pairs of electrodes on wPLI. Although the electrodes and pairs of electrodes showed significant differences, we did not find a consistent tendency across the frequency bands or analyses (Fig. 3).

3.3. Prognostic values using receiver operating characteristic (ROC) curves

To differentiate between groups F and R, we used ROC curves for each analysis with $p < 0.001$, using mean values in each frequency band for each patient (Table 2). The optimal operating point for each value at the maximum value of the Youden index was calculated from the ROC analysis, and the corresponding sensitivity and specificity were determined. The best prognostic value in group R based on area under curve was demonstrated to be

Table 1
Clinical data.

		Seizure-free (F) (n = 21)	Seizure-recurrence (R) (n = 7)	*p*-value
No. of females (%)		12 (57.1%)	5 (71.4%)	0.42
Gestational age < 37 weeks		5 (23.8%)	0 (0%)	0.21
Neonatal asphyxia		4 (19.0%)	0 (0%)	0.29
Etiology	**Unknown**	19	5	0.35
	Genetic	3	2	
Mean age at ES onset (SD), months[a]		5.7 (1.7)	4.3 (1.6)	0.09
Mean age at pretreatment EEG (SD), months[a]		6.8 (2.7)	5.3 (2.1)	0.19
Use of chloral hydrate on EEG recording		19 (90.5%)	5 (71.4%)	0.21
Developmental delay prior to ES onset		3 (14.3%)	2 (28.6%)	0.92
Other AEDs prior to ACTH[b]		21 (100%)	7 (100%)	
Treatment lag < 30 days before ACTH		13 (61.9%)	5 (71.4%)	0.51
Mean duration of ACTH (SD), days		23.8 (9.5)	23.1 (7.1)	0.86
Mean cumulative dose of ACTH (SD), mg/kg		0.27 (0.083)	0.33 (0.18)	0.45
Resolution of ES at the end of ACTH		21 (100%)	6 (85.7%)	0.25
Resolution of EEG abnormalities at the end of ACTH		13 (61.9%)	4 (57.1%)	0.58
Mean follow-up period after ACTH (SD), months		41.4 (25.8)	58.9 (25.0)	0.17

Patients' profiles were reported as numbers and percentages or as means and standard deviations. For group comparisons, we used Fisher's exact probability test and Welch's t-test, as appropriate.

Abbreviations: ES, epileptic spasms; SD, standard deviation; EEG, electroencephalography; AEDs, antiepileptic drugs; ACTH, adrenocorticotropic hormone.

[a] Age was corrected for prematurity (<37 weeks' gestation).

[b] Including vitamin B6.

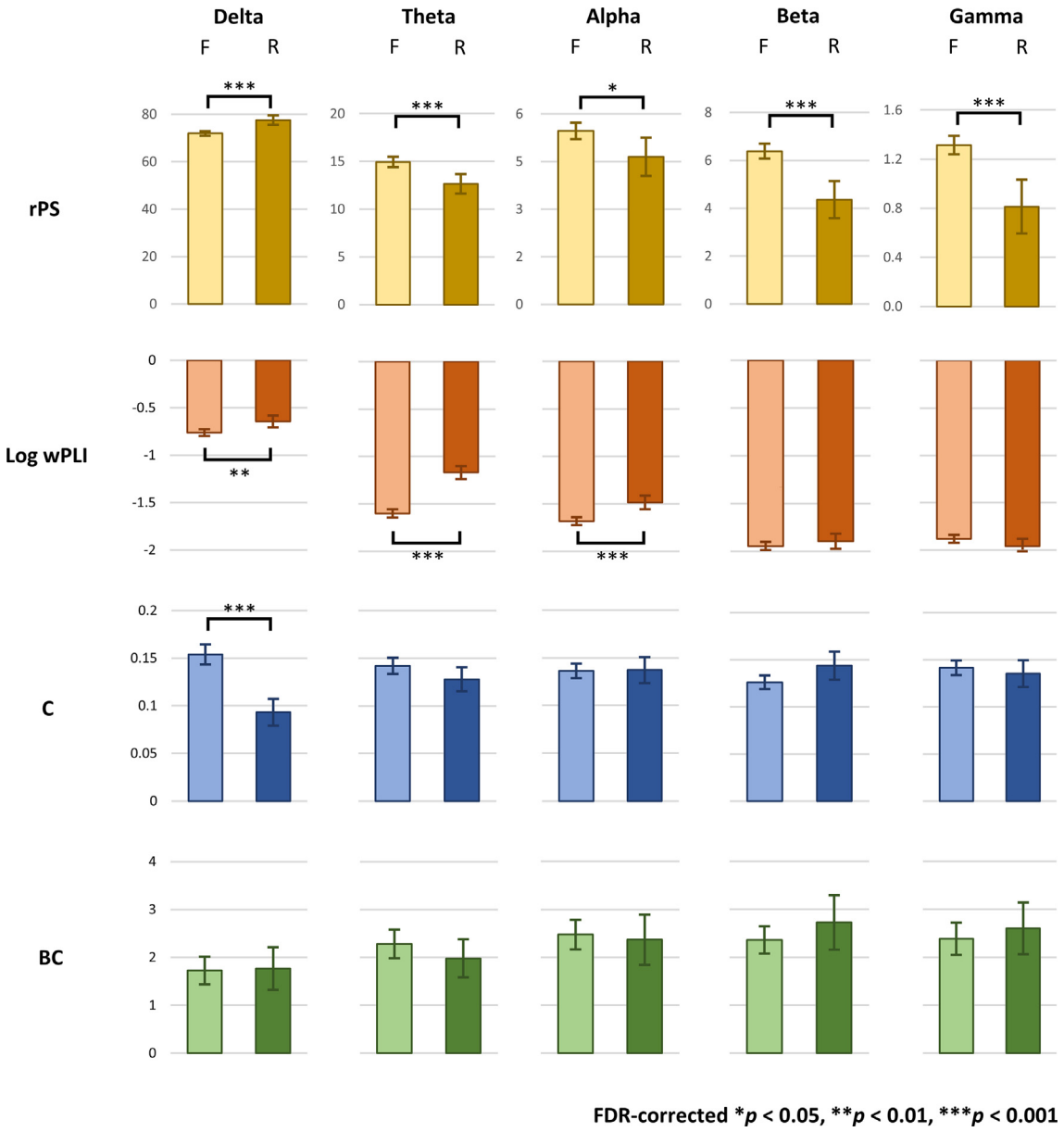

Fig. 2. Group differences with 95% CIs using two-way factorial ANOVA Bar graphs representing the mean value in each group and for each analysis. Estimates with FDR-corrected $p < 0.05$ are shown with asterisks. Significantly higher log wPLI values were identified in delta, theta, and alpha frequency bands in group R than in group F. The C in the delta frequency band was significantly lower in group R than in group F, although BC measures did not reveal significant differences across all frequency bands. *Abbreviations:* CIs, confidence intervals; ANOVA, analysis of variance; R, seizure-recurrence; F, seizure-free; FDR, false discovery rate; rPS, relative power spectrum; wPLI, weighted phase lag index; C, clustering coefficient; BC, betweenness centrality.

theta frequency band in log wPLI, with the sensitivity and specificity of 0.96 and 0.57, respectively.

4. Discussion

Our findings potentially identify robust prognostic factors for an early establishment of treatment strategies. The results of the analyses may provide a novel insight into the interpretation of the lower frequency bands on EEG in non-lesional IESS, which have been rarely mentioned in previous studies, and further highlight the subcortical pathological mechanisms. The present study comprised a highly homogeneous cohort compared to those of previous studies in terms of patients' age, treatment strategy, pretreatment EEG, and MRI findings.

4.1. EEG quantitative analysis for IESS

Several quantitative analyses for scalp EEG have been applied in clinical studies of IESS as methods that enable a more objective evaluation. As the occurrence of pretreatment hypsarrhythmia was not associated with treatment response in patients with ES (Demarest et al., 2017), mechanical quantitative analyses are required to predict outcomes objectively. Burroughs et al. clarified the higher rPS value in the delta frequency band in patients with IESS compared to controls (Burroughs et al., 2014). Since the EEG power in the delta band decreases during infantile period (Zhang et al., 2021), the increased rPS in the delta frequency band might indicate the immaturity of neural development in patients with intractable IESS.

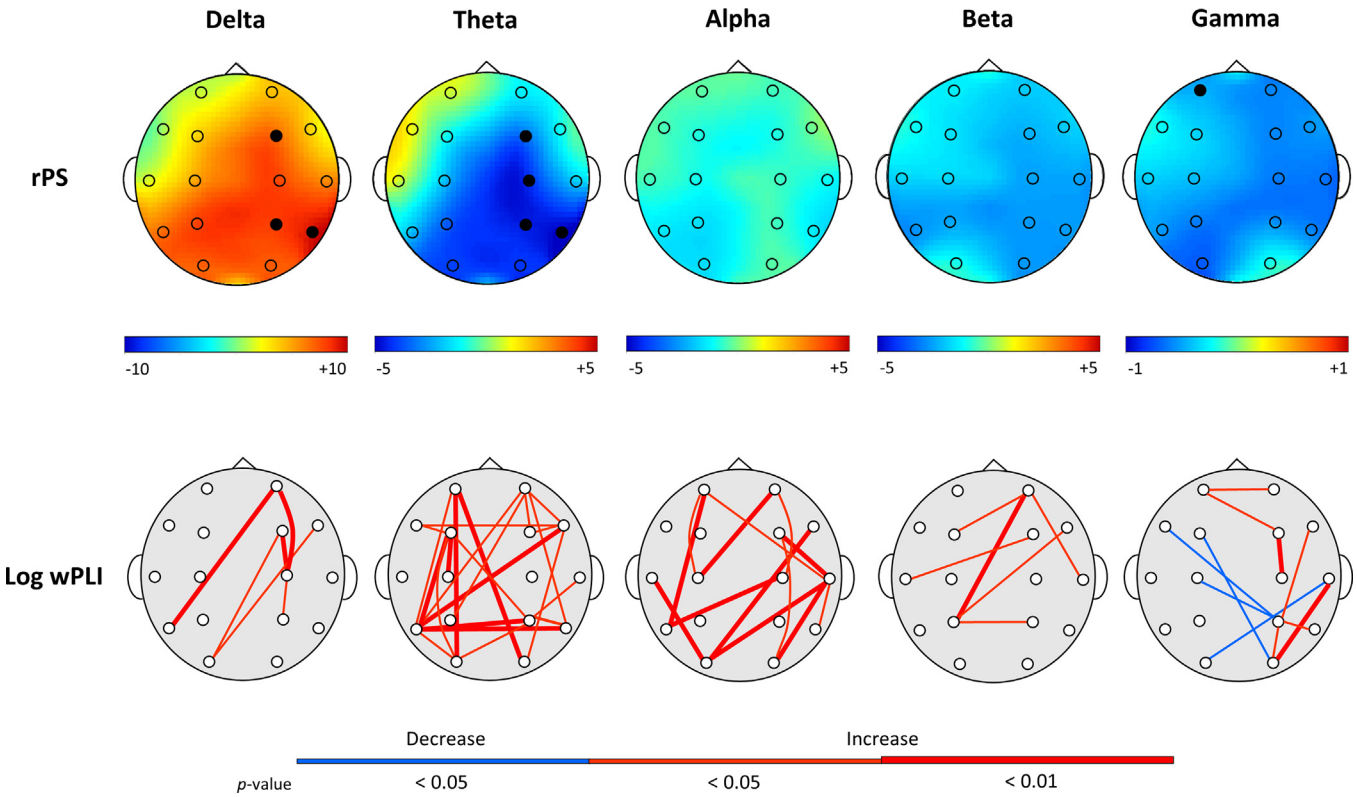

Fig. 3. Electrode maps representing the differences between groups in each frequency bands (superior view) The rPS topographic maps reveal the differences of mean relative power between groups (group R–F). The color calibration is shown under each figure. Electrodes with statistically significant differences identified via Welch's t-test are indicated by black circles. The log wPLI maps indicate the pairs of electrodes with statistically significant differences. The red line indicates increased functional connectivity, and blue line indicates lower connectivity in group R compared with group F. The line thickness represents the *p*-value using Welch's t-test. Note that the differences between groups are observed not locally but globally. *Abbreviations:* rPS, relative power spectrum; wPLI, weighted phase lag index; R, seizure-recurrence; F, seizure-free.

Table 2
Cutoff values for seizure recurrence using the receiver operating characteristic curves.

Analysis	Frequency band	AUC	Cutoff value	Sensitivity for seizure recurrence	Specificity for seizure recurrence
rPS	Delta	0.73	78.78	0.81	0.71
	Theta	0.73	12.96	0.76	0.71
	Beta	0.76	5.40	0.71	0.86
	Gamma	0.77	0.73	0.71	0.86
Log wPLI	Theta	0.83	−1.06	0.96	0.57
	Alpha	0.76	−1.50	0.78	0.86
C	Delta	0.80	0.093	0.91	0.71

Abbreviations: rPS, relative power spectrum; wPLI, weighted phase lag index; C, clustering coefficient; AUC, area under curve.

Notably, the present study aimed to clarify the characteristics of pretreatment EEG using quantitative analyses and revealed significant correlations between unfavorable outcomes and increased functional connectivity in the lower frequency bands. Previously, few studies have focused on the prognostic value of EEG functional connectivity analyses for IESS. Chu et al. demonstrated significantly higher complexity of pretreatment scalp EEG in AED responders than non-responders among patients with IESS caused by various etiologies (Chu et al., 2021). Similarly, another study revealed the tendency of strong broadband connectivity in patients with favorable seizure outcome, although it was not statistically significant due to small sample size and intragroup heterogeneity (Shrey et al., 2018). These authors hypothesized that a higher functional connectivity in pretreatment EEG may reflect a less impairment of brain functions in patients with favorable outcomes. However, they did not consider the differences among each frequency band.

The differences of the results between our study and the previous studies are as follows: higher relative power and functional connectivity in the lower frequency bands vs lower functional connectivity in patients with unfavorable outcomes might be attributable to the homogenous condition of "non-lesional" nature in our study. Previous studies included the patients with cortical lesions and revealed that the high-frequency component on intracranial (Iimura et al., 2018) and scalp EEG (Bernardo et al., 2020; Kobayashi et al., 2015; Baba et al., 2019; Nariai et al., 2017) indicated the strong cortical epileptogenesis. In our patients with non-lesional IESS, the subcortical dysfunction might be a dominant cause of the emergence of hypsarrhythmia, and increase rPS and functional connectivities in the lower frequency bands are more prominent compared to those in the previous studies.

4.2. Possible mechanisms for increased connectivity of lower frequency bands in IESS

According to a previous study, hypsarrhythmia can result from projections of the activated brainstem raphe area through raphe–

cortical interactions (Chugani, 2002). Japaridze et al. reported that the dynamic imaging of coherent sources with the randomized partial directed coherence method in EEG revealed a significant informational flow from the brainstem toward the putamen and cerebral cortex during delta activity on hypsarrhythmia in patients with IESS (Japaridze et al., 2013). Moreover, a similar upward flow was identified in patients with burst-suppression pattern, another form of EEG in early infantile DEEs (Japaridze et al., 2015). Comparing hypsarrhythmia and the electrodecremental phase, higher phase synchronization has been observed during the former phase, especially at the 3-Hz bandwidth (Nenadovic et al., 2018). Since these findings suggest that the burst phase of hypsarrhythmia is generated by the subcortical activity resulting in the high phase synchronization in lower frequency bands, we selectively analyzed this phase.

In group R, based on the analyses of differences between each pair of electrodes in wPLI, the abnormal functional connectivity in lower frequency bands increased rather globally than locally, and rather among distant electrodes, suggesting the influence of deep brain structures. A longitudinal diffusion tensor imaging study revealed reduced mean diffusivity in the dorsal brainstem and immature white matter, suggestive of cytotoxic edema, at the onset in WS of unknown etiology (Ogawa et al., 2018). The projections from the affected subcortical structures might result in the lower frequency activities diffusely synchronized on the cerebral cortices. In our study, the globally increased connectivity of the lower frequency bands in group R may also be associated with more severe dysfunction of the subcortical structures than in group F, thus resulting in the unfavorable outcomes following ACTH therapy.

Interestingly, the C in the delta frequency band was significantly lower in group R than in group F, and the theta frequency band also showed a similar tendency, in contrast to functional connectivity. A higher C likely reflects increased short-range connectivity, and increased BC reflects robust broad network. Higher frequency bands are more involved in establishing cognitive representation, whereas lower frequencies are more anatomically constrained (Rosch et al., 2018). The network in the developing infantile brain changes as it is dynamically modulated by local microcircuit and global network integration (Basset and Bullmore, 2006). We hypothesized that the results of the network analyses were influenced by the immaturity of our infantile cohort, and the C in the delta frequency band, an indicator of an anatomically primitive and local network, was more disorganized due to dysfunction of the subcortical structure in group R.

5. Limitations

The present study has some limitations. First, our analyses focused only on the burst phase of hypsarrhythmia. Frequent interictal epileptiform discharges are associated with a global increase in connection strength (Hu et al., 2020). When considering the pathogenesis of IESS, the suppression phase also plays an important role. Quantitative analyses comparing the burst and suppression phases may facilitate the penetration of the mechanism of periodic hypsarrhythmia.

Second, despite the multicenter retrospective design, our focus on the non-lesional nature resulted in a limited number of patients, especially in group R. A larger number of patients in group R might have elucidated the power spectrum, functional connectivity, or network in high-frequency bands, which implicates the refractoriness of IESS (Iimura et al., 2018; Bernardo et al., 2020; Wang et al., 2021; Uda et al., 2021; Kobayashi et al., 2015; Baba et al., 2019; Demarest et al., 2017). Meanwhile, since we applied the values of each electrode directly as variables, the significant differences between two outcome groups could more easily be identified.

To understand the pathogenesis and electrophysiological network of IESS, we must discuss the heterogeneity of its etiology. Fusco et al. advocated three different scenarios for ES: WS, DEEs, and ES in the context of focal epilepsies (Fusco et al., 2020). Our cohort included a patient with an *STXBP1* mutation, which indicates a close association with DEEs. However, as genetic variants are seldom distinguished at the onset of IESS, they do not significantly affect the selection of initial therapy.

6. Conclusion

The present study is important for predicting long-term outcomes in patients with non-lesional IESS despite the abovementioned limitations. We applied pretreatment scalp EEG recorded in routinely performed clinical settings, which can be utilized in hospitals without tertiary epilepsy units. Although ACTH therapy is certainly an important option for the temporal cessation of ES, even in refractory patients, it can be deleterious in some cases. The potential role of the present study is to distinguish the long-term prognosis for patients with non-lesional IESS in early stages and to provide treatment strategies other than ACTH therapy, including dietary and surgical therapies, for patients with unfavorable prognosis. Further analyses with larger sample sizes and extended etiologies may contribute to establishing more appropriate treatment strategies and obtaining a deeper understanding of the pathological mechanism of IESS.

Declarations of Interest

None.

Author contributions

S.K., T.O., and Y.M. contributed to the study conception and design. S.K., Y.M., M.M., K.Y., R.M., T.T., S.S., T.C., and S.H. contributed to data acquisition. S.K. and M.O. contributed to the processing and analysis of the EEG data. S.K. and T.O. contributed to the statistical analyses. S.K. contributed to drafting the manuscript and preparing the figures.

Funding

This work was supported by Grants-in-Aid for Scientific Research (Grant No JP19K17332) from the Japan Society for the Promotion of Science.

Data Availability Statement

All datasets and codes are available upon request from the Lead Contact.

Acknowledgements

We are thankful to the patients and families who participated in this study.

Appendix A. Supplementary material

Supplementary data to this article can be found online at https://doi.org/10.1016/j.clinph.2022.10.004.

References

Baba S, Vakorin VA, Doesburg SM, Nagamori C, Cortez MA, Honda R, et al. EEG before and after total corpus callosotomy for pharmacoresistant infantile spasms: Fast oscillations and slow-wave connectivity in hypsarrhythmia. Epilepsia 2019;60:1849–60. https://doi.org/10.1111/epi.16295.

Baram TZ, Mitchell WG, Snead OC, Horton EJ, Saito M. Brain-adrenal axis hormones are altered in the CSF of infants with massive infantile spasms. Neurology 1992;42:1171–5. https://doi.org/10.1212/wnl.42.6.1171.

Basset DS, Bullmore E. Small-world brain networks. Neuroscientist 2006;12:512–23. https://doi.org/10.1177/1073858406293182.

Benjamini Y, Hochberg Y. Controlling the false discovery rate: A practical and powerful approach to multiple testing. J R Stat Soc Series B Stat Methodol 1995;57:289–300.

Bernardo D, Nariai H, Hussain SA, Sankar R, Wu JY. Interictal scalp fast ripple occurrence and high frequency oscillation slow wave coupling in epileptic spasms. Clin Neurophysiol 2020;131:1433–43. https://doi.org/10.1016/j.clinph.2020.03.025.

Bitton JY, Desnous B, Sauerwein HC, Connolly M, Weiss SK, Donner EJ, et al. Cognitive outcome in children with infantile spasms using a standardized treatment protocol. A five-year longitudinal study. Seizure 2021;89:73–80. https://doi.org/10.1016/j.seizure.2021.04.027.

Burroughs SA, Morse RP, Mott SH, Holmes GL. Brain connectivity in West syndrome. Seizure 2014;23:576–9. https://doi.org/10.1016/j.seizure.2014.03.016.

Chu YJ, Chang CF, Weng WC, Fan PC, Shieh JS, Lee WT. Electroencephalography complexity in infantile spasms and its association with treatment response. Clin Neurophysiol 2021;132:480–6. https://doi.org/10.1016/j.clinph.2020.12.006.

Chugani HT. Pathophysiology of infantile spasms. Adv Exp Med Biol 2002;497:111–21. https://doi.org/10.1007/978-1-4615-1335-3_13.

Daida A, Hamano S, Hayashi K, Nonoyama H, Ikemoto S, Hirata Y, et al. Comparison of adrenocorticotropic hormone efficacy between aetiologies of infantile spasms. Seizure 2021;85:6–11. https://doi.org/10.1016/j.seizure.2020.12.008.

Demarest ST, Shellhaas RA, Gaillard WD, Keator C, Nickels KC, Hussain SA, et al. The impact of hypsarrhythmia on infantile spasms treatment response: Observational cohort study from the National Infantile Spasms Consortium. Epilepsia 2017;58:2098–103. https://doi.org/10.1111/epi.13937.

Fusco L, Serino D, Santarone ME. Three different scenarios for epileptic spasms. Epilepsy Behav 2020;113:107531. https://doi.org/10.1016/j.yebeh.2020.107531.

Gul Mert G, Herguner MO, Incecik F, Altunbasak S, Sahan D, Unal I. Risk factors affecting prognosis in infantile spasm. Int J Neurosci 2017;127:1012–108. https://doi.org/10.1080/00207454.2017.1289379.

Hu DK, Mower A, Shrey DW, Lopour BA. Effect of interictal epileptiform discharges on EEG-based functional connectivity networks. Clin Neurophysiol 2020;131:1087–98. https://doi.org/10.1016/j.clinph.2020.02.014.

Iimura Y, Jones K, Takada L, Shimizu I, Koyama M, Hattori K, et al. Strong coupling between slow oscillations and wide fast ripples in children with epileptic spasms: Investigation of modulation index and occurrence rate. Epilepsia 2018;59:544–54. https://doi.org/10.1111/epi.13995.

Imperatori LS, Betta M, Cecchetti L, Canales-Johnson A, Ricciardi E, Siclari F, et al. EEG functional connectivity metrics wPLI and wSMI account for distinct types of brain functional interactions. Sci Rep 2019;9:8894. https://doi.org/10.1038/s41598-019-45289-7.

Japaridze N, Muthuraman M, Moeller F, Boor R, Anwar AR, Deuschl G, et al. Neuronal networks in West syndrome as revealed by source analysis and randomized partial directed coherence. Brain Topogr 2013;26:157–70. https://doi.org/10.1007/s10548-012-0245-y.

Japaridze N, Muthuraman M, Reinicke C, Moeller F, Anwar AR, Mideksa KG, et al. Neuronal networks during burst suppression as revealed by source analysis. PLoS One 2015;10:e0123807.

Kobayashi K, Akiyama T, Oka M, Endoh F, Yoshinaga H. A storm of fast (40–150Hz) oscillations during hypsarrhythmia in West syndrome. Ann Neurol 2015;77:58–67. https://doi.org/10.1002/ana.24299.

Knupp KG, Coryell J, Nickels KC, Ryan N, Leister E, Loddenkemper T, et al. Response to treatment in a prospective National Infantile Spasms Cohort. Ann Neurol 2016;79:475–84. https://doi.org/10.1002/ana.24594.

Mytinger JR, Hussain SA, Islam MP, Millichap JJ, Patel AD, Ryan NR, et al. Improving the inter-rater agreement of hypsarrhythmia using a simplified EEG grading scale for children with infantile spasms. Epilepsy Res 2015;116:93–8. https://doi.org/10.1016/j.eplepsyres.2015.07.008.

Nariai H, Beal J, Galanopoulou AS, Mowrey WB, Bickel S, Sogawa Y, et al. Scalp EEG ictal gamma and beta activity during infantile spasms: Evidence of focality. Epilepsia 2017;58:882–92. https://doi.org/10.1111/epi.13735.

Nenadovic V, Whitney R, Boulet J, Cortez MA. Hypsarrhythmia in epileptic spasms: Synchrony in chaos. Seizure 2018;58:55–61. https://doi.org/10.1016/j.seizure.2018.03.026.

Ogawa C, Kidokoro H, Fukasawa T, Yamamoto H, Ishihara N, Ito Y, et al. Cytotoxic edema at onset in West syndrome of unknown etiology: A longitudinal diffusion tensor imaging study. Epilepsia 2018;59:440–8. https://doi.org/10.1111/epi.13988.

Ortiz E, Stingl K, Münssinger J, Braun C, Preissl P, Belardinelli P. Weighted phase lag index and graph analysis: Preliminary investigation of functional connectivity during resting state in children. Comput Math Methods Med 2012;2012:186353. https://doi.org/10.1155/2012/186353.

Paprocka J, Malkiewicz J, Palazzo-Michalska V, Nowacka B, Kuźniak M, Kopyta I. Effectiveness of ACTH in patients with infantile spasms. Brain Sci 2022;12:254. https://doi.org/10.3390/brainsci12020254.

Pavone P, Polizzi A, Marino SD, Corsello G, Falsaperla R, Marino S, et al. West syndrome: A comprehensive review. Neurol Sci 2020;41:3547–62. https://doi.org/10.1007/s10072-020-04600-5.

Pegg EJ, Taylor JR, Laiou P, Richardson M, Mohanraj R. Interictal electroencephalographic functional network topology in drug-resistant and well-controlled idiopathic generalized epilepsy. Epilepsia 2021;62:492–503. https://doi.org/10.1111/epi.16811.

Peng BW, Li XJ, Wu WX, Zeng YR, Liao YT, Hou C, et al. The possible role of hypothalamus-pituitary-adrenal dysfunction in epileptic spasms. Seizure 2020;81:145–50. https://doi.org/10.1016/j.seizure.2020.07.032.

Peraza LR, Asghar AUR, Green G, Halliday DM. Volume conduction effects in brain network inference from electroencephalographic recordings using phase lag index. J Neurosci Methods 2012;207:189–99. https://doi.org/10.1016/j.jneumeth.2012.04.007.

Richardson MP. Large scale brain models of epilepsy: Dynamics meets connectomics. J Neurol Neurosurg Psychiatry 2012;83:1238–48. https://doi.org/10.1136/jnnp-2011-301944.

Riikonen R. Infantile spasms: Outcome in clinical studies. Pediatr Neurol 2020;108:54–64. https://doi.org/10.1016/j.pediatrneurol.2020.01.015.

Riikonen R, Lähdetie J, Kokki H. ACTH treatment of infantile spasms: Low-moderate- versus high-dose natural versus synthetic ACTH – a retrospective cohort study. Pediatr Neurol 2020;111:46–50. https://doi.org/10.1016/j.pediatrneurol.2020.06.010.

Rosch R, Baldeweg T, Moeller F, Baier G. Network dynamics in the healthy and epileptic developing brain. Netw Neurosci 2018;2:41–59. https://doi.org/10.1162/NETN_a_00026.

Rubinov M, Sporns O. Complex network measures of brain connectivity: Uses and interpretations. Neuroimage 2010;52:1059–69. https://doi.org/10.1016/j.neuroimage.2009.10.003.

Shrey DW, McManus OK, Rajaraman R, Ombao H, Hussain SA, Lopour BA, et al. Strength and stability of EEG functional connectivity predict treatment response in infants with epileptic spasms. Clin Neurophysiol 2018;129:2137–48. https://doi.org/10.1016/j.clinph.2018.07.017.

Uda T, Kuki I, Inoue T, Kunihiro N, Suzuki H, Uda H, et al. Phase-amplitude coupling of interictal fast activities modulated by slow waves on scalp EEG and its correlation with seizure outcomes of disconnection surgery in children with intractable nonlesional epileptic spasms. J Neurosurg Pediatr 2021;27:572–80. https://doi.org/10.3171/2020.9.PEDS20520.

van Diessen E, Diederen SJH, Braun KPJ, Jansen FE, Stam CJ. Functional and structural brain network in epilepsy: What have we learned? Epilepsia 2013;54:1855–65. https://doi.org/10.1111/epi.12350.

Velísek L, Jehle K, Asche S, Velísková J. Model of infantile spasms induced by N-methyl-D-aspartic acid in prenatally impaired brain. Ann Neurol 2007;61:109–19. https://doi.org/10.1002/ana.21082.

Vinck M, Oostenveld R, van Wingerden M, Battaglia F, Pennartz CMA. An improved index of phase-synchronization for electrophysiological data in the presence of volume-conduction, noise and sample-size bias. Neuroimage 2011;55:1548–65. https://doi.org/10.1016/j.neuroimage.2011.01.055.

Wang W, Li H, Yan J, Zhang H, Li X, Zheng S, et al. Automatic detection of interictal ripples on scalp EEG to evaluate the effect and prognosis of ACTH therapy in patients with infantile spasms. Epilepsia 2021;62:2240–51. https://doi.org/10.1111/epi.17018.

Xia M, Wang J, He Y. BrainNet Viewer: A network visualization tool for human brain connections. PLoS One 2018;8:e68910.

Zhang H, Wang C, Yang T, Phua KS, Ng VSH, Law ECN. Infant EEG band power analysis at 6 months and 18 months. Annu Int Conf IEEE Eng Med Biol Soc 2021;2021:6353–6. https://doi.org/10.1109/EMBC46164.2021.9629872.

Zuberi SM, Wirrell E, Yozawitz E, Wilmshurst JM, Specchio N, Riney K, et al. ILAE classification and definition of epilepsy syndromes with onset in neonates and infants: Position statement by the ILAE Task Force on Nosology and Definitions. Epilepsia 2022;63:1349–97. https://doi.org/10.1111/epi.17239.